Appl. Phys. A 74 [Suppl.], S1077–S1079 (2002) / Digital Object Identifier (DOI) 10.1007/s003390101192

Applied Physics A
Materials
Science & Processing

Vacancy ordering in nanosized maghemite from neutron and X-ray powder diffraction

Z. Somogyvári[1], E. Sváb[1,*], G. Mészáros[1], K. Krezhov[2], I. Nedkov[3], I. Sajó[4], F. Bourée[5]

[1] Research Institute for Solid State Physics and Optics, Hungarian Academy of Sciences, 1525 Budapest, POB 49, Hungary
[2] Institute for Nuclear Research and Nuclear Energy, Bulgarian Academy of Sciences, 72 Tzarigradsko Chaussee, 1784 Sofia, Bulgaria
[3] Institute of Electronics, Bulgarian Academy of Sciences, 72 Tzarigradsko Chaussee, 1784 Sofia, Bulgaria
[4] Institute of Chemistry, Hungarian Academy of Sciences, 1525 Budapest, POB 17, Hungary
[5] Laboratoire Léon Brillouin (CEA-CNRS), CEA/Saclay, 91 191 Gif-sur-Yvette, France

Received: 16 July 2001/Accepted: 24 October 2001 –

Abstract. Powder neutron and X-ray diffraction patterns of nanocrystalline needle-shaped maghemite (γ-Fe_2O_3) particles with average size 240 nm × 30 nm show the presence of superstructure peaks indicating a long-range ordering of the cation vacancies. The crystallographic parameters, the characteristics of the tetragonal distortion, and the vacancy distribution were determined in space group $P4_12_12$ by multiprofile Rietveld refinement.

PACS: 61.10.Nz; 61.12.Ld; 61.66.Fn

With recent advances in nanotechnology, maghemite (γ-Fe_2O_3) became of considerable current interest for preparation of high-density recording media in magneto-optical devices [1–3]. The structure of maghemite is closely related to that of the inverse spinel Fe_3O_4, but the network of iron atoms is partially depleted containing only ferric ions. It is widely accepted in the literature from X-ray [4–6], neutron diffraction [7], Mössbauer [5, 8] and magnetization studies [2, 9] that the cation vacancies are distributed on the octahedral cation sites in the molecular formula of $(Fe^{3+})[Fe^{3+}_{5/3}\square_{1/3}]O_4$, where $\square$ denotes a vacancy. The further ordering of vacancies forms a structure basically similar to that of $LiFe_5O_8$ (space group $P4_332$) with vacancies concentrated on the site corresponding to Li [10].

Both X-ray [4–6] and neutron diffraction [7] studies revealed the appearance of several weak extra lines in the diffraction patterns; recently the tetragonal space group $P4_12_12$ was found [6] to identify the lattice symmetry. However, the quantitative analysis of the tetragonal ordering and of the possibly attendant structure distortions has not yet been done.

In the present study we performed a multiprofile Rietveld refinement on neutron and X-ray diffraction patterns, focusing our attention to describe the structural details corresponding to the correct space group, and the long-range cation vacancy ordering on a nanocrystalline sample with needle-shaped grains.

*Corresponding author. (Fax: +36-1/3922589, E-mail: svab@szfki.hu)

1 Experimental

γ-Fe_2O_3 acicular nanoparticles were prepared by oxidizing in air at 250 °C colloidal Fe_3O_4 obtained by soft solution processing [11]. Scanning electron microscopy pictures have shown nanocrystaline needle-shaped particles with an average size 240 nm × 30 nm (with a length to minor-axis ratio of 8 : 1), while diffraction analysis revealed traces of hematite (α-Fe_2O_3).

Neutron-diffraction measurements were carried out using the medium-resolution PSD diffractometer ($\lambda = 1.0577$ Å) at Budapest and the high-resolution 3T2 diffractometer ($\lambda = 1.2251$ Å) at LLB, Saclay at ambient temperature using a cylindrical sample geometry. The X-ray measurement was obtained by a Philips powder diffractometer with Cu K_α radiation in reflection geometry. The obtained powder patterns were refined by the multiprofile Rietveld method using the program package Fullprof [12].

2 Results and discussion

Evaluated multiprofile refinements of the neutron and X-ray patterns are presented in Figs. 1 and 2. Tetragonal ordering is manifested by the occurrence of weak additional lines as shown on an enlarged scale in the inserted figures.

The initial average configuration was refined using the description corresponding to space group $P4_332$ with a ferrimagnetic spin arrangement. Except for the weak tetragonal extra reflections, all the cubic reflections were generated with satisfactory agreement. The results obtained for the atomic coordinates, for the isotropic temperature factors, and for the iron occupancies are summarized in Table 1. A strong preference of the vacancies for the 4b octahedral site was established. However, a small amount of vacancies were evaluated for the remaining 12*d* octahedral and even for the 8c tetrahedral sites. The sum of the occupation factors became lower than would follow from the ideal 2 : 3 Fe–O ratio corresponding to γ-Fe_2O_3, indicating the presence of lattice hydrogen, which decreases the average neutron-scattering length of the sublattices more strongly than the vacancies due to

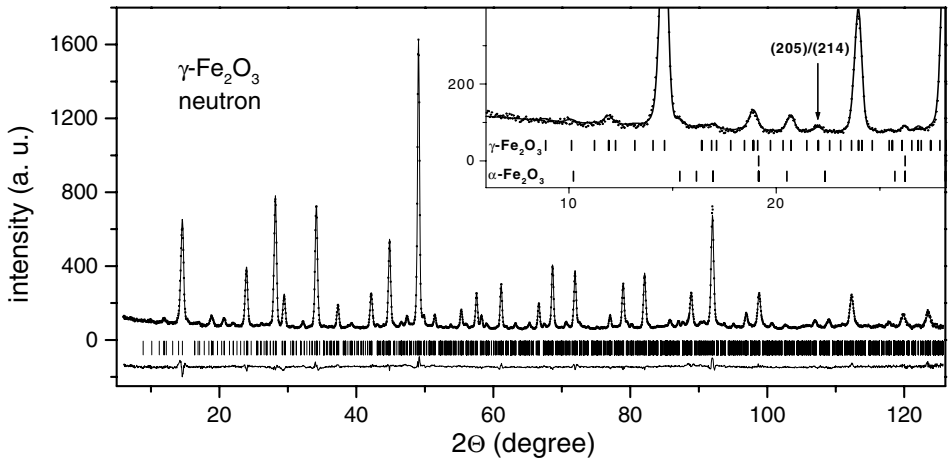

Fig. 1. Neutron-diffraction pattern ($\lambda = 1.2251$ Å) and Rietveld refinement of γ-Fe_2O_3 in space group $P4_12_12$. In the *inserted figure* the *top row* of indexes designates the reflections of maghemite, while the *two bottom rows* of indexes correspond to the nuclear and magnetic contributions of α-Fe_2O_3, respectively. The *arrow* indicates the most intense tetragonal extra reflection ($R_N = 3.3\%$, $R_M = 3.8\%$)

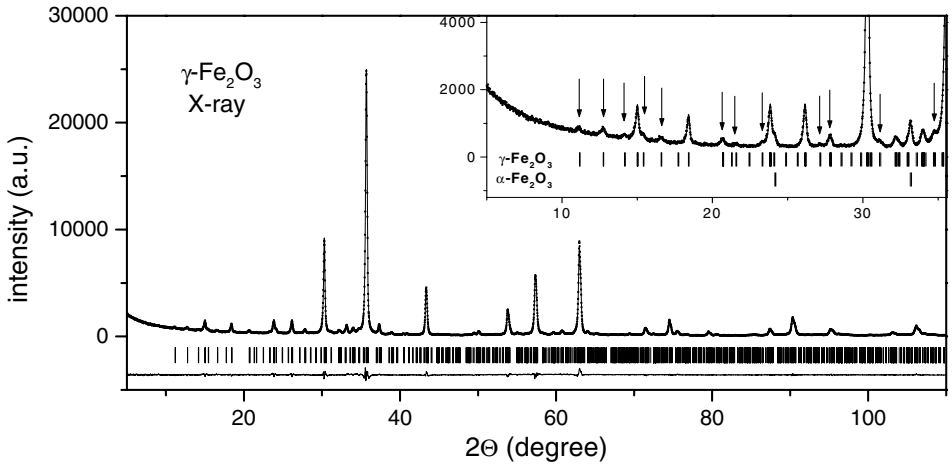

Fig. 2. X-ray diffraction pattern (Cu K_α) for γ-Fe_2O_3 and Rietveld refinement in space group $P4_12_12$. The significant tetragonal extra reflections are indicated by *arrows* in the *enlarged figure*. The contribution of α-Fe_2O_3 is also indexed ($R = 3.6\%$)

Table 1. Crystallographic parameters in the basic $P4_332$ space group, $a = 8.3438(1)$ Å (notation: -o – octahedral and -t – tetrahedral)

Wickoff position	x/a	y/a	z/a	B_{iso} (Å^2)	Occ_{Fe} (%)
Fe 12*d*-o	0.125	0.3650(2)	0.8850(2)	0.66(3)	95(1)
Fe 4*b*-o	0.625	0.625	0.625	0.66(3)	40(1)
Fe 8*c*-t	0.9947(2)	0.9947(2)	0.9947(2)	0.44(3)	97(1)
O 8*c*	0.8630(4)	0.8630(4)	0.8630(4)	0.88(4)	
O 24*e*	0.1179(4)	0.1297(4)	0.3809(3)	0.88(4)	

its negative scattering length. From the electroneutrality law the composition was established to be $Fe_{2.60}H_{0.20}\square_{0.20}O_4$. Another indicator of hydrogen was the appearance of its significant characteristic incoherent scattering in the neutron-diffraction pattern as compared to measurements on reference samples. In further data analysis we supposed that vacancies and H ions behave in the same way; thus we mention only vacancies in the following description.

With the aim of a deeper insight into the maghemite structure the resultant atomic positions were transformed to the tetragonal $P4_12_12$ space group proposed earlier [6]. The refinement of the tetragonal unit-cell parameters gave the values $a = 8.3498(1)$ and $c = 24.9960(6)$ Å, i.e. $c/a = 2.994(1)$, showing a slight distortion of the basic cubic lattice. The lowering of the symmetry splits the positions of space group $P4_332$ into several nonequivalent positions with eight or four Wickoff multiplicities ($12d \rightarrow 8b \times 4$, $4a \times 1$, $4b \rightarrow 8b \times 1$, $4a \times 1$, $8c \rightarrow 8b \times 3$) raising the number of independent atomic coordinates from six to 62. The overall fit in the tetragonal $P4_12_12$ space group proved to describe satisfactorily the extra peaks as demonstrated in Figs. 1 and 2. However, the slight discrepancies between calculated and measured patterns are attributed to the *hkl*-dependent line broadening arising from the needle shape of the grains. As the splitting of the main cubic reflections is very small, the size effect results in the formation of complicated *hkl*-dependent profiles.

Some of the most important structural parameters characterizing the tetragonal distortion, the vacancy distribution, and the magnetic-moment values are summarized in Table 2.

The occupancies of the sites that arose from the 12*d* cubic position proved to be highly correlated; thus they were constrained to give a homogenous cation distribution, leading to an average vacancy content of 8%. Remarkable changes occurred in the ordering of vacancies between the 8*b* and 4*a* octahedrally surrounded sites (originated from the 4*b* site of the $P4_332$ space group), resulting in 82% and 15% vacancy content, respectively. The occupation factors of the tetrahedral cation sites did not change substantially as compared to the $P4_332$ description, still showing the presence of a relatively small amount of vacancies (6%) without special ordering on the three nonequivalent tetrahedral cation sublattices.

Table 2. Structural parameters characterizing the tetragonal distortion

$P4_332$	$P4_12_12$			
Fe–O distance (Å)	Fe–O distance (Å)		Occ_{Fe} (%)	M (μ_B)
Fe_{12d}: 2.022(4)	$Fe_{8b\times4,4a\times1}$:	2.03(3)	92(1)	3.54(6)
Fe_{4b}: 2.126(4)	$Fe_{8b\times1}$:	2.20(5)	18(1)	3.54(6)
	$Fe_{4a\times1}$:	2.01(3)	85(1)	3.54(6)
Fe_{8c}: 1.882(4)	$Fe_{8b\times3}$:	1.87(3)	94(1)	−4.03(7)

The rather different values for the Fe–O first-neighbor distances for the vacancy-poor (2.022 Å) and vacancy-rich (2.126 Å) octahedral cation positions obtained from the refinement done in $P4_332$ space group indicates that vacancies have a strong influence on their local surroundings. Thus the changes in the vacancy ordering must eventually lead to an alteration of the atomic configuration. In our case the great number of free coordinates made it impossible to refine the structure without any constraints on the site positions. Hence, for all the cation–oxygen first-neighbor distances soft distance constraints were applied, which prevented the close-packed basic structure from being immoderately destroyed.

The changes in the average first-neighbor distances are in accordance with the expectations. The average distances remained the same inside the uncertainties of the refinement except in the case of the split 4b site, where the Fe_{4a}–O average distance decreased to 2.01 Å, which is very similar to the distance corresponding to the other likewise-occupied octahedral sites, while the polyhedron surrounding the almost fully vacant Fe_{8b} atom expanded further to give an average first-neighbor distance of 2.20 Å.

A pronounced reduction in the ferrimagnetic sublattice moments was observed when comparing our results to the values published by Greaves [7]. These changes are partially attributed to the nanosize effect, as Greaves examined acicular particles with dimensions of $700 \times 100\,nm^2$, and the published critical size determined from saturation magnetization measurements for developing superparamagnetism is in the order of 40 nm [13].

Acknowledgements. This work was supported by Hungarian Grant No. OTKA-29402, by the EC ICAI-CT-2000-70026, HPRI-CT-1999-00099 and HPRI-CT-1999-00032 programmes, and by Bulgarian Grant No. NFNI-816.

References

1. G. Bate: *Ferromagnetic Materials*, ed. by E.P. Wolfarth (North-Holland, Amsterdam 1980) pp. 381–507
2. E. Schmidbauer, R. Keller: J. Magn. Magn. Mater. **152**, 99 (1996)
3. R.H. Kodama, A.E. Berkowitz: Phys. Rev. B **59**, 6321 (1999)
4. G.W. van Oosterhout, C.J.M. Rooijans: Nature **181**, 44 (1958)
5. K. Haneda, A.H. Morrish: Solid State Commun. **22**, 779 (1977)
6. N. Shmakov, G.N. Kryukova, S.V. Tsibula, A.I. Chuvilin, L.P. Solovyeva: J. Appl. Crystallogr. **28**, 141 (1995)
7. C. Greaves: J. Solid State Chem. **49**, 325 (1983)
8. R.J. Armstrong, A.H. Morrish, G.A. Sawatzky: Phys. Lett. **23**, 414 (1966)
9. J.M.D. Coey, D. Khalafalla: Phys. Status Solidi A **11**, 229 (1972)
10. P.B. Braun: Nature **179**, 1123 (1952)
11. I. Nedkov: NATO Sci. Ser. II Math. Phys. Chem. **8**, 115 (2000)
12. J. Rodriguez-Carvajal: FULLPROF vers. 2k (2001) [http://www-llb.cea.fr/winplotr/winplotr.htm]
13. A.E. Berkowitz, W.J. Schuele: J. Appl. Phys. **39**, 1261 (1968)